



Spatial expression of the *FGFR2b* splice isoform and its prognostic significance in endometrioid endometrial carcinoma

Asmerom T Sengal¹ , Deborah Smith², Cameron E Snell², Samuel Leung³, Aline Talhouk⁴, Elizabeth D Williams¹, Jessica N McAlpine⁴ and Pamela M Pollock^{1*} 

¹School of Biomedical Sciences, Faculty of Health, Queensland University of Technology (QUT) located at the Translational Research Institute (TRI), Brisbane, Australia

²Mater Pathology, Mater Research and University of Queensland, Brisbane, Australia

³Department of Pathology and Laboratory Medicine, Genetic Pathology Evaluation Centre, University of British Columbia, Vancouver, BC, Canada

⁴Department of Gynaecology and Obstetrics, Division of Gynaecologic Oncology, University of British Columbia, Vancouver, BC, Canada

*Correspondence to: Pamela M Pollock, Endometrial Cancer Laboratory, School of Biomedical Sciences, Faculty of Health, Queensland University of Technology located at the Translational Research Institute (TRI), PA Hospital Campus, 37 Kent St, Woolloongabba, Brisbane 4102, Australia. E-mail: pamela.pollock@qut.edu.au

Abstract

Endometrial carcinoma (EC) is the most common gynecological malignancy and fibroblast growth factor receptor 2 (FGFR2) is a frequently dysregulated receptor tyrosine kinase. FGFR2b and FGFR2c are the two main splice isoforms of FGFR2 and are normally localized in epithelial and mesenchymal cells, respectively. Previously, we demonstrated that *FGFR2c* mRNA expression was associated with aggressive tumor characteristics, shorter progression-free survival (PFS), and disease-specific survival (DSS) in endometrioid ECs (EECs). The objectives of this study were to investigate the spatial expression of FGFR2b in normal and hyperplasia with and without atypia of human endometrium and to assess the prognostic significance of FGFR2b expression in EC. *FGFR2b* and *FGFR2c* mRNA expression was evaluated in normal (proliferative [$n = 10$], secretory [$n = 15$], and atrophic [$n = 10$] endometrium), hyperplasia with and without atypia ($n = 19$) as well as two patient cohorts of EC samples (discovery [$n = 78$] and Vancouver [$n = 460$]) using isoform-specific BaseScope RNA *in situ* hybridization assays. Tumors were categorized based on *FGFR2* isoform expression (one, both, or neither) and categories were correlated with clinicopathologic markers, molecular subtypes, and clinical outcomes. The *FGFR2b* splice isoform was exclusively expressed in the epithelial compartment of normal endometrium and hyperplasia without atypia. We observed *FGFR2c* expression at the basalis layer of glands in 33% (3/9) of hyperplasia with atypia. In patients with EEC, FGFR2b+/FGFR2c- expression was found in 48% of the discovery cohort and 35% of the validation Vancouver cohort. In univariate analyses, tumors with FGFR2b+/FGFR2c- expression had longer PFS (hazard ratio [HR] 0.265; 95% CI 0.145–0.423; log-rank $p < 0.019$) and DSS (HR 0.31; 95% CI 0.149–0.622; log-rank $p < 0.001$) compared to tumors with FGFR2b-/FGFR2c+ expression in the large EEC Vancouver cohort. In multivariable Cox regression analyses, tumors with FGFR2b+/FGFR2c- expression were significantly associated with longer DSS (HR 0.37; 95% CI 0.153–0.872; log-rank $p < 0.023$) compared to FGFR2b-/FGFR2c+ tumors. In conclusion, FGFR2b+/FGFR2c- expression is associated with favorable clinicopathologic markers and clinical outcomes suggesting that FGFR2b could play a role in tailoring the management of EEC patients in the clinic if these findings are confirmed in an independent cohort.

Keywords: alternative splicing; biomarkers; endometrial carcinoma; uterine cancer; endometrial hyperplasia; FGFR2b isoform; FGFR2c isoform; molecular subtypes; RNA ISH

Received 19 January 2022; Revised 19 May 2022; Accepted 7 June 2022

No conflicts of interest were declared.

Introduction

Endometrial carcinoma (EC) is the most prevalent female pelvic cancer in developed nations and its incidence is increasing annually [1]. Traditionally, ECs

were classified broadly into type I and type II [2]. Type I ECs are the most frequently diagnosed (~80%), endometrioid in histology [endometrioid EC (EEC)], and generally considered to have a favorable clinical course. Type II ECs are non-EECs (NEEC)

including serous, clear cell, and carcinosarcomas and they are associated with a poor survival outcome.

In 2013, the Cancer Genome Atlas (TCGA) network identified four molecular subtypes with distinct genomic profiles that have prognostic significance [3]. Subsequently, these molecular subtypes were validated using surrogate immunohistochemistry (IHC) markers and limited mutation analyses by Dutch [4,5] and Canadian [6,7] research groups with slight modifications in nomenclature to align with the biomarker signatures. These molecular subtypes are polymerase ϵ -exodomain mutated (POLE EDM)/ultra-mutated (excellent prognosis), microsatellite instability/mismatch repair-deficient (MMRd) (intermediate prognoses), copy-number low/wild-type p53 (p53wt) (intermediate prognoses), and copy-number high/p53 mutant/abnormal (p53abn) (worst prognosis). Clinical management and de-escalation of treatment based on molecular risk stratification are currently being assessed in prospective clinical trials including PORTEC-4a (NCT03469674) [8] and TAPER (NCT04705649). However, most of the newly diagnosed EC patients (~80%) fall into the MMRd and p53wt molecular subtypes with 'intermediate prognosis' highlighting the need for additional prognostic biomarkers within these groups, as well as the identification of potential predictive markers for more effective therapies in both the adjuvant and metastatic settings.

Alternative splicing in exons 8 and 9 of fibroblast growth factor receptor 2 (FGFR2) produces two isoforms, FGFR2b and FGFR2c [9]. These are localized in epithelial and mesenchymal cells, respectively [9]. FGFR2 plays different physiologic and pathologic roles in various cellular process including cell growth, migration, invasion, differentiation, and angiogenesis [9]. FGFR2 is dysregulated via different mechanisms (mutation, amplification, fusion, and isoform switching) and contributes to carcinogenesis of several cancers [10]. FGFR inhibition with small-molecule inhibitors is currently approved for the treatment of cancers with *FGFR* fusions, including infigratinib and pemigatinib in cholangiocarcinoma and erdafitinib in locally advanced or metastatic urothelial carcinoma, and these FGFR inhibitors are being trialed in multiple additional cancer types.

Recently, we have developed a novel RNA *in situ* hybridization (ISH) assay that detects *FGFR2b* and *FGFR2c in situ* at single-cell resolution while preserving the morphologic context of the tumor [11]. *FGFR2c* mRNA was evaluated in 460 EC patients from the Vancouver cohort and expression was documented in 40% of the samples [11]. *FGFR2c* expression was associated with poor clinicopathologic prognostic markers and shorter progression-free survival (PFS) and disease-specific

survival (DSS). Integration of *FGFR2c* expression with clinicopathologic parameters (International Federation of Gynaecology and Obstetrics [FIGO] grade and FIGO stage) and molecular subtypes was able to further refine and improve the risk stratification and potentially avoid under/over treatment in EEC patients [11].

It has been reported that the FGFR2b isoform has a tumor suppressive role [12] and expression of the FGFR2b isoform has been associated with good prognostic markers in liver cancer [13] and clear cell renal cell carcinoma [14]. In a transgenic mouse model, mice with conditional deletion of *Fgfr2b* in epidermal keratinocytes developed a spectrum of pathological abnormalities in the skin including squamous carcinoma [15]. Conditional knockout (KO) of *Fgfr2b* in the murine uterine epithelium driven by Cre recombinase under the control of the *Wnt7a* promoter showed that abnormal development and proliferation and crowding of endometrial glands in mice and consequently *Fgfr2b* KO mice are infertile [16]. While our previous report focused on FGFR2c and its association with poor prognosis, the objective of this investigation is to evaluate the spatial and temporal expression of both FGFR2b and FGFR2c isoforms in apparently normal human endometrium at different phases of the menstrual cycle, as well as in hyperplasia (with and without atypia) and clinically annotated ECs using *FGFR2* splice isoform-specific RNA ISH probes. We also evaluated if the retained *FGFR2b* expression played a role in identifying tumors with improved prognosis in the molecularly profiled Vancouver cohort.

Materials and methods

Patients

Formalin-fixed paraffin-embedded (FFPE) clinical patient samples, in the form of tissue microarrays (TMAs; UT 242a, and UT 801), representing hyperplasia with and without atypia and ECs with different stages and grades were obtained from US Biomax (Rockville, MD, USA). Where applicable, clinicopathologic data including age, clinical diagnosis, histologic type, FIGO grade, and stage were also provided by commercial suppliers.

Whole sections of hysterectomy samples were obtained from the Mater Hospital after ethical approval (Mater REF # HREC/15/MHS/127 and Queensland University of Technology [QUT] HREC REF # 1500000169). FFPE whole serial sections (4 μ m thickness) were obtained from samples representing atrophic endometrium ($n = 10$), secretory endometrium ($n = 15$), proliferative endometrium ($n = 10$), and ECs ($n = 25$). The

apparently normal endometrium samples were obtained from women who underwent a hysterectomy for benign conditions including uterine myoma, adenomyosis, and uterine prolapse, as part of surgical management for cervical or ovarian tumors that had not extended to the endometrium and were not treated with radiotherapy and/or chemotherapy or following a prophylactic hysterectomy in patients with germline *BRCA1/2* gene mutations. These patients were operated on between January 2015 and March 2018 at the Mater Hospital, Brisbane, Australia. None of the patients included in this study had received preoperative neoadjuvant therapy. The histologic type, myometrial invasion, lymphovascular space invasion (LVSI), lymph node metastasis, and histologic grade were assessed by an anatomic pathologist. The staging was performed according to the FIGO (2009) version [17]. Ethical clearance to analyze the Vancouver cohort of EC patients' samples ($n = 460$, TMAs) from the McAlpine Laboratory in Canada was obtained (reference # UBC-H09-00939 and QUT HREC #1800000670). This cohort of EC patient samples was used for discovery and confirmation of Proactive Molecular Risk Classifier for Endometrial Cancer (ProMisE) [6,7] and all clinical and molecular parameters were defined as reported previously [11]. The REporting recommendations for tumor MARKer (REMARK) criteria [18] were followed as previously reported [11].

IHC staining and scoring

FGFR2 IHC staining was performed manually as previously published using a non-isoform-specific anti-FGFR2 antibody (Cat# Ab58201, Abcam, Cambridge, UK) [11]. IHC was scored using two parameters; intensity of stain and percentage of positive tumor cells using a semi-quantitative immune-reactivity histologic scoring method (H-score) as previously published [11,19]. In brief, H-score was calculated as follows: $H\text{-score} = \sum(P_{1-3})$, where P is the percentage of positive tumor cells, I is the intensity of staining (I_1 – weak, I_2 – moderate, and I_3 – strong intensity), and the maximum H-score is 300.

Determination of *FGFR2* isoforms using BaseScope RNA ISH

We employed the BaseScope RNA ISH assay that has been previously developed, optimized, and validated by our laboratory to detect the *FGFR2b* and *FGFR2c* isoforms [11,20]. In brief, we utilized custom-designed probes from Advanced Cell Diagnostic (ACD) (Newark, CA, USA): (1) a human-specific probe (1ZZ) (BA-Hs-FGFR2-tv2-E7E8) that targets an exon 7–8 junction (NM_022970.3, 1,578–1,622 bp) to detect the 'FGFR2b'

epithelial isoform and (2) a human-specific probe (BA-Hs-FGFR2-tv1-E7E9) that targets an exon 7–9 junction (NM_000141.4, 1,580–1,619 bp) to detect the 'FGFR2c mRNA' mesenchymal isoform. Each batch run of the assay included an FGFR2b-positive biological control (cell pellets from Ishikawa cells transduced with *FGFR2b*), an *FGFR2c*-positive biological control (AN3CA cells with endogenous *FGFR2c* expression confirmed by RT-PCR), a positive control targeting the peptidylprolyl isomerase B (PPIB) housekeeping gene to assess RNA quality, and a negative technical control DaB (a probe targeting a bacterial gene). All samples were scored by two independent observers (ATS and PMP), blinded to patient outcome data. Scoring was performed as previously described [11]. In brief, score 0, no signal dots or ≤ 1 dot signal per 10 tumor cells at $\times 40$ objective magnification; score 1+, 1–3 signal dots per cell; score 2+, 4–10 signal dots per tumor cell; score 3+, >10 signal dots per cell with <10 cluster dots; and score 4+, >10 signal dots per cell and ≥ 10 cluster dots at $\times 20$ objective magnification. Finally, patient samples were grouped into four groups based on the *FGFR2* isoform status expression as follows: (1) *FGFR2b*+/*FGFR2c*- (tumor samples with exclusive FGFR2b expression of any RNA ISH score of 1–4); (2) *FGFR2b*+/*FGFR2c*+ (tumor samples that express both FGFR2b and FGFR2c with any RNA ISH score of 1–4); (3) *FGFR2b*-/*FGFR2c*+ (tumor samples that exclusively express *FGFR2c* of any RNA ISH score 1–4); and (4) *FGFR2b*-/*FGFR2c*- (tumor samples negative for both *FGFR2b* and *FGFR2c*, RNA ISH score 0 but positive for PPIB). Samples negative for PPIB were excluded from further statistical analyses.

Computational analysis for the determination of *FGFR2* isoforms in the TCGA RNA-seq UCEC cohort

Computational determination of *FGFR2* isoforms was performed using exon–exon junction counts as previously published [11]. To determine the expression of each isoform in each sample, we combined the number of reads spanning the 7–8 junction (Chr10:123278344 to chr10:123279492) and the 8–10 junction (Chr10:123274834 to chr10:123278195) for a total of *FGFR2b* read counts. Similarly, we combined the number of reads spanning the 7–9 junction (Chr10:123276978 to chr10:123279492) and the 9–10 junction (Chr10:123274834 to chr10:123276832) to identify the total *FGFR2c* read counts. To determine the expression ratio, we computed the number of exon–exon junction reads including exon 8 over the junction reads and exon 9, as described previously [14]. Given that TCGA samples generally had $>66\%$ tumor cellularity and we

saw low *FGFR2c* expression in the stroma with the BaseScope assay, we defined a ratio of 1.5-fold of $[7-9 + 9-10]/[7-8 + 8-10]$ to identify tumors with isoform switching from *FGFR2b* to *FGFR2c*. Similarly, a ratio of 1.5-fold of $[7-8 + 8-10]/[7-9 + 9-10]$ was considered *FGFR2b* expression. A ratio >0.67 to <1.5 for either *FGFR2c* $[7-9 + 9-10]/[7-8 + 8-10]$ or *FGFR2b* $[7-8 + 8-10]/[7-9 + 9-10]$ was defined as expressing both *FGFR2b* and *FGFR2c* isoforms. Any single exon junction read count of <3 was considered 'no callout' (negative for both *FGFR2b* and *FGFR2c* isoforms).

To evaluate gene expression patterns within the three categories of *FGFR2* isoforms (*FGFR2c+*, *FGFR2b+*, and *FGFR2b-IFGFR2c-*), mRNA expression reads per million kilobyte of selected genes including hormone receptors (progesterone receptor and estrogen receptor [PR and ER]), known epithelial cell markers, mesenchymal cell markers that have been previously published in EC [21,22] and other cancers [14,23], and cognate FGF ligands to *FGFR2b* and *FGFR2c* as well as the major *FGFR2* splice regulatory protein (epithelial splice regulatory protein 1 [ESRP1]) were downloaded from the cBioPortal of TCGA-uterine corpus endometrial carcinoma (UCEC) and exported into excel. RNA-seq data of these selected genes were log transformed and normalized, and then clustered and visualized as heat maps using the modified version of Gene Cluster 3.0 software [24].

Statistical analyses

All data analysis was performed using IBM, SPSS (version 26) (Chicago, IL, USA). Chi-squared tests were used for more than two categorical variables and Fisher's exact test was used for dichotomized categorical variables. Where applicable, pairwise analyses were performed to compare the four categories of *FGFR2* isoform status with each variable category and correction for multiple comparisons was performed using the Bonferroni method. Time-to-event analyses were calculated as previously published [11]. Kaplan–Meier method was used to sketch survival curves (overall survival [OS], DSS, and PFS) and *P* values were determined using the log-rank test (LRT). Cox regression proportional hazard models were used to explore the prognostic significance of each factor/variable as previously described [11]. In brief, factors with $p < 0.10$ were included in a multivariate Cox regression model with a stepwise forward method for inclusion in the final analysis. In the last step, significant factors from the forward selection model ($p < 0.05$) were included in the final Cox regression model together with established clinicopathologic prognostic factors:

myometrial invasion (negative or $<50\%$ versus $>50\%$), LVSI (negative versus positive), FIGO grade (1–2 versus 3), FIGO stage (I/II versus III/IV), ProMisE molecular subgroups (MMRd versus p53wt, POLE versus p53wt, and p53abn versus p53wt), and *FGFR2* isoform status. A bootstrap method taking an arbitrary 1,000 samples was used to internally validate all models of analysis. All reported *P* values were two tailed and based on the likelihood ratio test, where $p < 0.05$ was defined as statistically significant.

Results

Bright-field chromogenic BaseScope RNA ISH was employed to determine *FGFR2b* and *FGFR2c* isoforms in normal endometrium of different cyclic phases, precursor hyperplasia, and a discovery cohort of ECs. Our *in situ* analyses of *FGFR2b* and *FGFR2c* isoforms in secretory phase ($n = 15$), proliferative phase ($n = 10$), and atrophic inactive endometrium ($n = 10$) showed *FGFR2b* expression exclusively in the epithelial compartment of apparently normal endometrium (Figure 1A–C). High *FGFR2b* expression was observed in the epithelial cells of secretory phase endometrium (Figure 1A) and very low expression in atrophic inactive endometrium (Figure 1C) concordant with its protein expression (Figure 1D). A significant difference in *FGFR2* expression ($p < 0.0001$) (both mRNA and protein) was observed among secretory, proliferative, and atrophic endometrium (Figure 1E). We observed a similar pattern of exclusive *FGFR2b* isoform expression within normal cervical and colon epithelia samples (supplementary material, Figure S1). *FGFR2c* signal was not evident in the normal endometrial epithelial compartment; however, occasionally, a few signal dots were observed in the stromal compartment of normal endometrium (Figure 2A).

FGFR2b was expressed in the epithelial compartment in 9/10 (90%) hyperplasia without atypia and 8/9 (88.9%) hyperplasia with atypia (Figure 2B,C). *FGFR2c* isoform was not expressed in the epithelial compartment but a few scattered signal dots were evident in the stroma of simple hyperplasia (Figure 2B, right panel). In a subset of atypical hyperplasia specimens (3/9), several cells at the basal layer of the tumor showed *FGFR2c* expression in addition to high signal in the stroma (Figure 2C, right panel).

In the current study, we aimed to investigate the role of *FGFR2b* in EEC prognosis and risk stratification. In order to assess this, we categorized *FGFR2* expression into four categories: *FGFR2b+IFGFR2c-*, *FGFR2b+IFGFR2c+*, *FGFR2b-IFGFR2c+*, and *FGFR2b-IFGFR2c-*.

In a discovery cohort of 78 cases from commercial EC TMAs ($n = 55$) and whole section hysterectomy

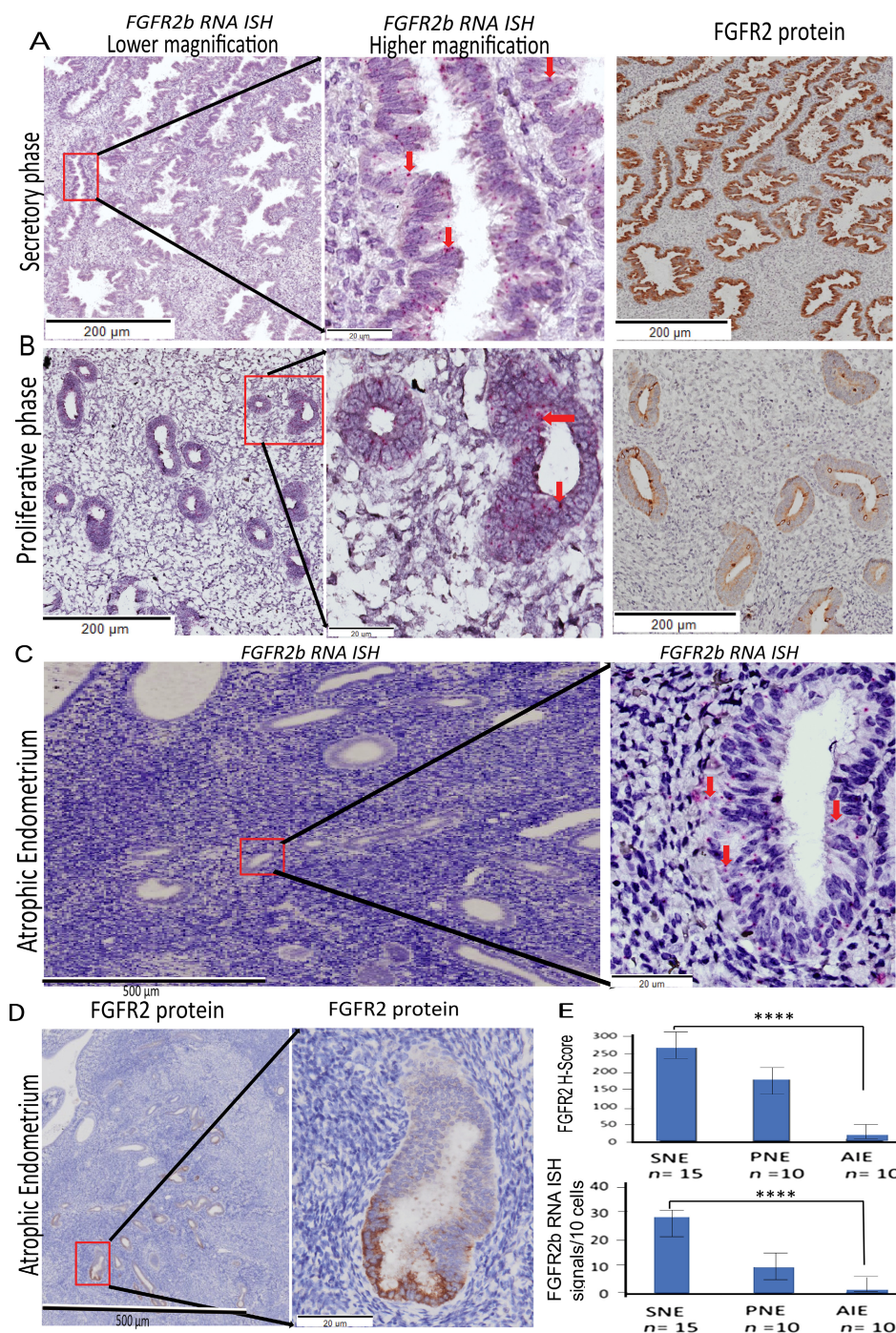


Figure 1. Representative images illustrating the temporal and spatial expression of *FGFR2b* mRNA and FGFR2 protein in apparently normal human endometrium. *FGFR2b* mRNA and FGFR2 protein in (A) secretory phase and (B) proliferative phase. (C) *FGFR2b* mRNA in atrophic inactive endometrium from a postmenopausal woman. (D) FGFR2 protein in atrophic inactive endometrium. Red boxes indicate the area magnified in adjacent images. Red arrows indicate *FGFR2b* mRNA in epithelial cells. (E) Bar graph demonstrating the pattern of FGFR2 protein expression (top) and *FGFR2b* mRNA (bottom) in normal endometrium at different phases of the cycle and in postmenopausal women with atrophied endometrium. **** $p < 0.0001$, error bar indicates standard error of the mean (SEM). AIE, atrophied inactive endometrium; PNE, proliferative phase of normal endometrium; SNE, secretory phase of normal endometrium. Scale bars, 500, 200, and 20 μm .

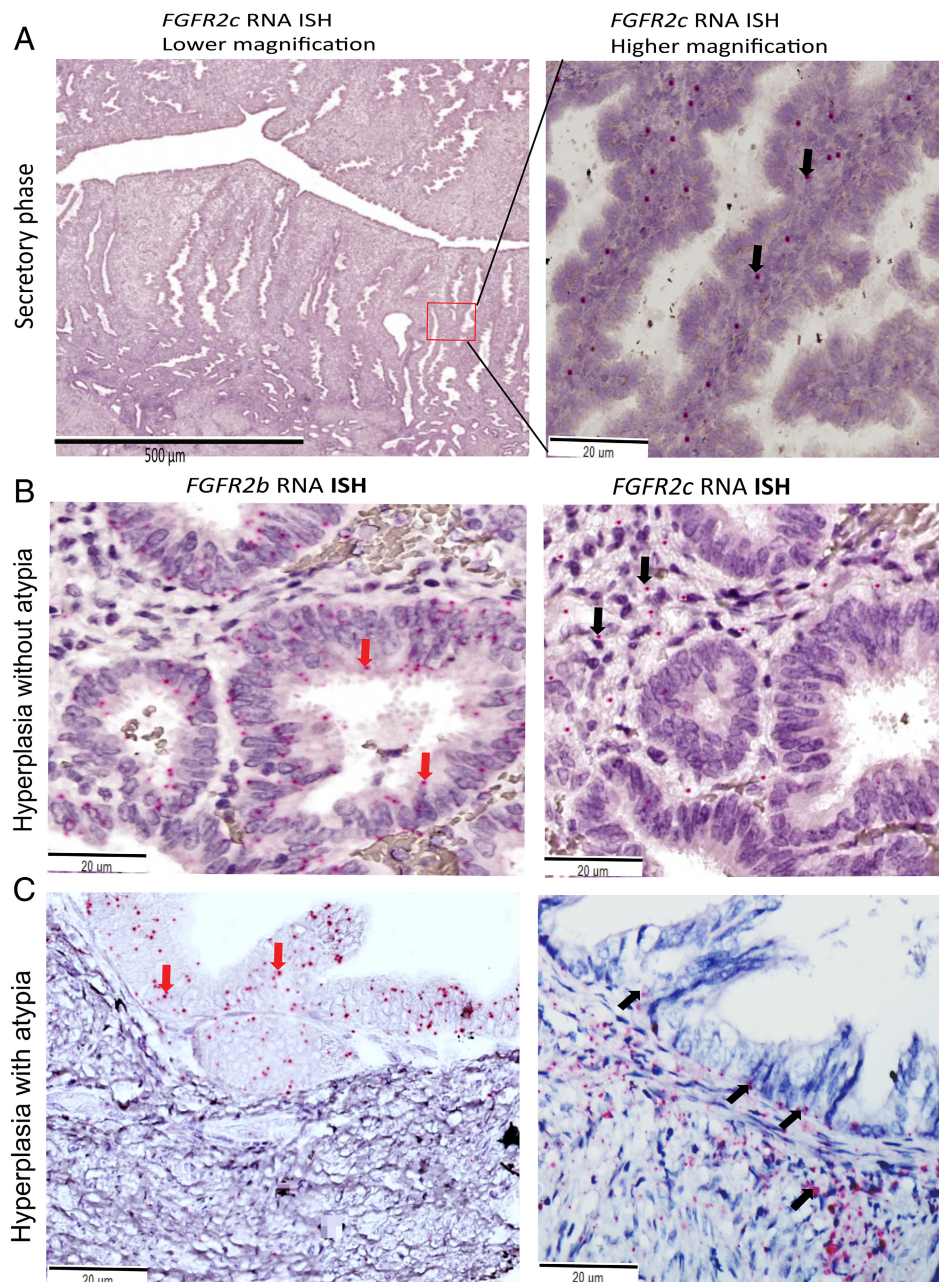


Figure 2. Pattern of *FGFR2b* and *FGFR2c* expression in representative normal secretory phase endometrium, hyperplasia without atypia, and hyperplasia with atypia. (A) *FGFR2c* isoform expression in the stroma of secretory phase endometrium (lower magnification [left panel] and higher magnification [right panel]). (B, C) *FGFR2b* isoform expression in the epithelial compartment of a hyperplasia without atypia and hyperplasia with atypia respectively (left panels) and *FGFR2c* expression in the stroma in serial section (right panel). Red box indicates the area in magnified view. Red arrows indicate *FGFR2b* RNA ISH signal dots in the epithelial compartment and black arrows indicate *FGFR2c* RNA ISH signal in the stroma. Note that some epithelial cells at the base of the gland (black arrows) in atypical hyperplasia also express *FGFR2c*, which could represent transformed malignant cells. Scale bars, 500, 200, and 20 μm.

samples ($n = 25$) from the Mater Hospital, we observed *FGFR2b*+/*FGFR2c*- expression in 33/78 (42.3%) EC samples, expression of *FGFR2b*+/*FGFR2c*+ in 10/78

(12.8%) ECs, expression of *FGFR2b*-/*FGFR2c*+ in 27/78 (34.6%) samples, and 8/78 (10.3%) tumors had no *FGFR2* expression (*FGFR2b*-/*FGFR2c*-).

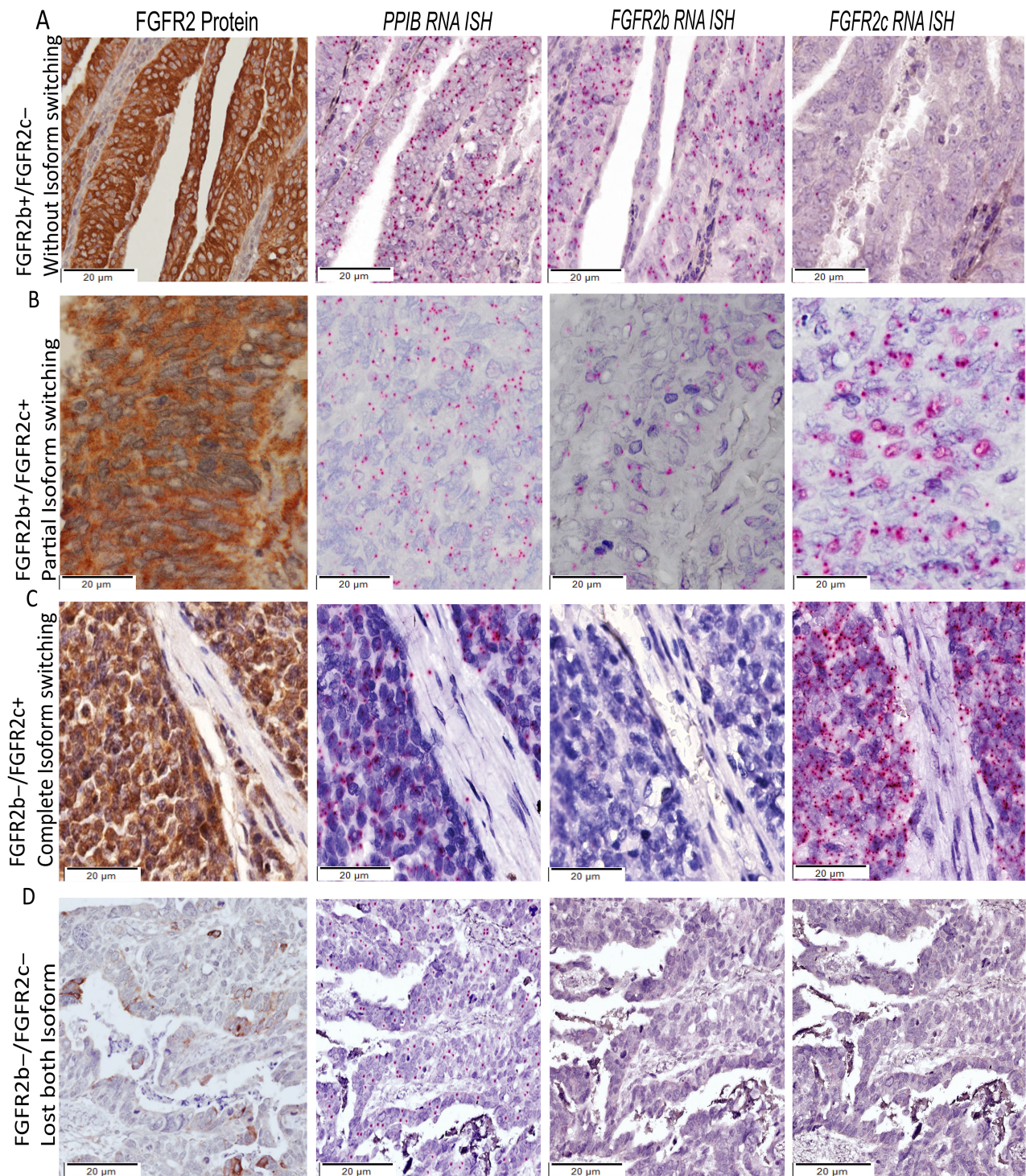


Figure 3. Representative micrograph images of the four classes of *FGFR2* isoforms in endometrial cancer. Serial sections from endometrial cancer samples of four women representing the four patterns of *FGFR2* isoform expression status. (A) Grade 1 (well-differentiated) EEC expressing only the *FGFR2b* isoform. (B) Grade 3 EEC expressing both *FGFR2b* and *FGFR2c* isoforms. (C) Grade 3 EEC expressing only the *FGFR2c* isoform. (D) Grade 2 EEC negative for both *FGFR2b* and *FGFR2c* isoforms.

Representative images from EEC specimens showing the four patterns of expression are presented in Figure 3. The association of *FGFR2* isoform status with clinicopathologic characteristics from the discovery cohort is provided in supplementary material, Table S1. Notably, in this discovery cohort, *FGFR2b+ / FGFR2c-* expression was significantly associated with endometrioid histology ($p < 0.0001$), well-differentiated EC ($p < 0.008$), early stage ($p < 0.001$), low/intermediate European Society of Medical Oncology (ESMO) risk group ($p < 0.01$), and with superficial (<50%) myometrial invasion ($p < 0.054$) (supplementary material, Table S1).

The confirmation cohort from Vancouver that was previously assessed for *FGFR2c* expression was then further

evaluated for *FGFR2b* expression. In this study, we restricted our report to EEC as *FGFR2* mutations primarily occur in EEC rather than NEEC [3,25] and our previous investigation indicated that *FGFR2c* has no prognostic significance in NEEC [11]. *FGFR2b+ / FGFR2c-* expression was identified in 105/302 (35%) EECs (Table 1 and Figure 4). The association of four categories of *FGFR2* isoform status and clinicopathologic, ESMO risk factors, and molecular subtypes in EEC from the Vancouver cohort is summarized in Table 1. In the Vancouver cohort, corrected pairwise multiple comparison analyses showed that *FGFR2b+ / FGFR2c-* isoform expression was significantly higher in tumors with FIGO grade 1/2, superficial (<50%) myometrial invasion, high ER and PR expression,

Table 1. Association between *FGFR2* isoform status and clinicopathologic and molecular subtypes in EEC in the Vancouver cohort

Clinicopathologic variables	<i>FGFR2</i> isoform status in EEC				Total N = 302	P value*
	<i>FGFR2b+ / FGFR2c-</i> (a) n = 105 (35%)	<i>FGFR2b+ / FGFR2c+</i> (b) n = 54 (18%)	<i>FGFR2b- / FGFR2c-</i> (c) n = 48 (16%)	<i>FGFR2b- / FGFR2c+</i> (d) n = 95 (31%)		
Age (years) <60	45 (43%)	17 (31.5%)	24 (50%)	32 (34%)	117 (39%)	0.12
Age (years) ≥60	60 (57%)	37 (68.5%)	24 (50%)	60 (63%)	182 (60%)	
Missing	0	0	0	3 (3%)	3 (1%)	
BMI < 25	24 (25%)	20 (40%)	14 (29%)	24 (30%)	82 (30%)	0.561
BMI 25–30	23 (24%)	12 (24%)	8 (16.5%)	20 (25%)	63 (23%)	
BMI ≥ 30	49 (51%)	18 (36%)	22 (46%)	36 (45%)	125 (46%)	
Missing	9 (8.6%)	4 (8%)	4 (8%)	15 (16%)	32 (11%)	
Grade 1/2	85 (80.2%) b c d	25 (46%)	27 (54%) d	28 (30%)	165 (55%)	0.0001
Grade 3	21 (19.8%)	29 (54%) a	20 (42%) a	64 (68%) a c	134 (44%)	
Missing	0	0	1 (2%)	2 (2%)	2 (1)	
MI neg or <50%	75 (71%) c d	38 (70%)	25 (51%)	48 (54%)	186 (63%)	0.023
MI > 50%	30 (29%)	16 (30%)	22 (47%)	41 (46%) a b	109 (37%)	
Missing	0	0	1 (2%)	6 (6.3%)	7 (2%)	
LVSI neg	71 (68%)	34 (63%)	25 (51%)	50 (52%)	180 (63%)	0.269
LVSI pos	30 (28%)	19 (35%)	19 (41%)	36 (39%) a	104 (37%)	
Missing	3 (3%)	1 (2%)	4 (8%)	9 (9.5%)	17 (5.6%)	
PR < 1%	14 (13%)	6 (11%)	16 (33%) a b	19 (20%) a b	55 (18%)	0.0001
PR > 1–50%	72 (67%) d	30 (56%) d	24 (50%) d	27 (29%)	163 (54%)	
PR > 50%	20 (19%)	16 (29.6%)	7 (15%)	21 (23%)	64 (21%)	
Unknown	1 (1%)	2 (4%)	1 (2%)	16 (17%)	20 (7%)	
ER negative	3 (3%) b c d	11 (21%) a	9 (20%) a	16 (18%) a	39 (14%)	0.0001
ER low	67 (68%) b d	22 (42%)	31 (67%) d	36 (40%)	156 (54%)	
ER high	29 (29%)	20 (38%)	6 (13%)	38 (42%) a c	93 (32%)	
Stage I/II	91 (86%)	49 (91%)	36 (77%)	70 (79%)	246 (83%)	0.139
Stage III/IV	15 (14%)	5 (9%)	11 (23%) a b	19 (21%) a b	50 (17%)	
ESMO risk low	59 (56%) b d	17 (32%)	19 (40%)	19 (21%)	114 (38%)	0.0001
ESMO risk intermediate	23 (22%)	17 (32%)	11 (23%)	30 (32.6%)	81 (27%)	
ESMO risk high	24 (23%)	20 (37%)	17 (36%)	43 (47%) a	104 (35%)	
<i>POLE</i>	11 (10%)	6 (11%)	4 (9%)	12 (13%)	33 (11%)	0.001
p53wt	66 (62%) b c d	24 (45%)	24 (51%)	38 (42%)	152 (51%)	
MMRd	27 (25%)	21 (40%) a d	16 (34%)	23 (25%)	87 (29%)	
p53abn	3 (3%)	2 (4%)	3 (6%)	18 (20%) a b c	26 (9%)	

The significance level for two-sided test (a, b, c, and d) is $p < 0.05$. Tests are adjusted for all pairwise comparisons within a stratum of each innermost sub-table using the Bonferroni correction.

BMI, body mass index; ESMO, ESMO endometrial cancer risk group; MI, myometrial invasion; neg, negative; p53, tumor protein 53; p53abn, null/misense p53 mutation; p53wt, wild-type p53; pos, positive.

*P value (pairwise over strata) was determined using Pearson's chi-squared test or Fisher's exact test for dichotomous variables. P values of <0.05 are indicated in bold. Cases with missing values were removed from analysis.

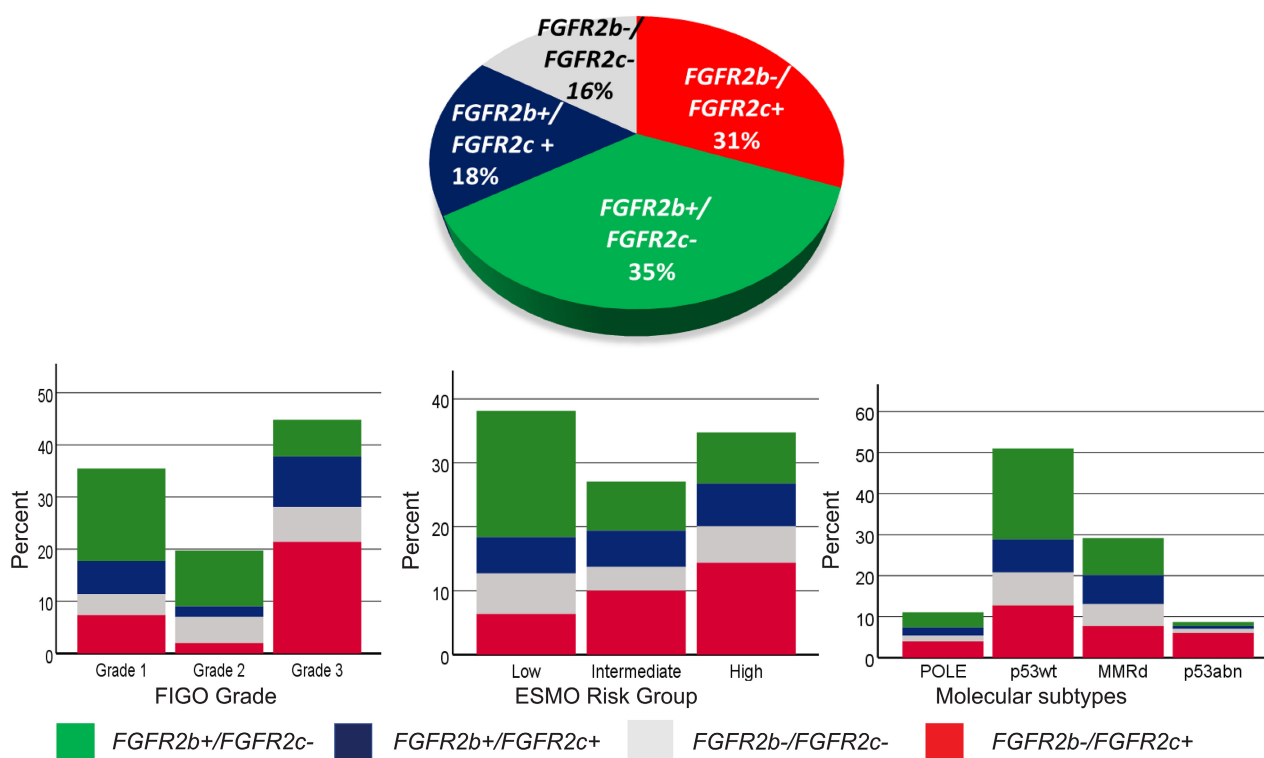


Figure 4. Distribution of *FGFR2* isoform expression by ESMO risk group, FIGO grade, and molecular subtype in EEC in the Vancouver cohort. The proportion of four groups of *FGFR2* isoforms (pie chart) and distribution by FIGO grade, ESMO risk group, and molecular subtypes (lower bar graph) in EEC.

low/intermediate ESMO risk group, and p53wt molecular subtypes compared to tumors with *FGFR2b+*/*FGFR2c+* and *FGFR2b-*/*FGFR2c+* expression (Table 1, variables with significant *P* values are indicated by small letters a, b, c, and d).

The 5-year DSSs of EEC patients in the Vancouver cohort for *FGFR2b+*/*FGFR2c-*, *FGFR2b-*/*FGFR2c-*, *FGFR2b+*/*FGFR2c+*, and *FGFR2b-*/*FGFR2c+* were 89, 72, 67% and 56%, respectively. In univariable Cox regression analyses, *FGFR2b+*/*FGFR2c-* tumors were significantly associated with longer PFS (hazard ratio [HR] 0.265; 95% CI 0.145–0.423; LRT *P* value [LRTP] <0.019), DSS (HR 0.31; 95% CI 0.149–0.622; LRTP <0.001), and OS (HR 0.48; 95% CI 0.298–0.781; LRTP <0.003) compared to *FGFR2b-*/*FGFR2c+* tumors in EECs (Table 2 and Figure 5A). Further corrected pairwise multiple comparison survival analyses among the four patterns of *FGFR2* isoform expression indicated that women with *FGFR2b+*/*FGFR2c-* expression had longer DSS and PFS compared to women with *FGFR2b+*/*FGFR2c+* and *FGFR2b-*/*FGFR2c+* (supplementary material, Table S2). In multivariable Cox regression analyses adjusting for known confounding prognostic factors (myometrial invasion,

FIGO grade, and stage and molecular subtype), tumors with *FGFR2b+*/*FGFR2c-* expression remained significantly associated with longer DSS (HR 0.37; 95% CI 0.153–0.872; LRTP <0.023) and OS (HR 0.71; 95% CI 0.409–0.921; LRTP <0.045) and showed a trend toward significance for PFS compared to *FGFR2b-*/*FGFR2c+* (Table 3).

Kaplan–Meier curve analyses also demonstrated that *FGFR2b+*/*FGFR2c-* tumors had better prognosis than *FGFR2b-*/*FGFR2c+* which can further discern the outcome of low/intermediate and high-risk groups within EECs (Figure 5B,C). Furthermore, when Kaplan–Meier curve analyses were performed by stratifying EECs by the molecular subtype, it was evident that *FGFR2b+*/*FGFR2c-* tumors showed better outcomes than *FGFR2b-*/*FGFR2c+* tumors in particular within the MMRd, p53wt, and p53 abnormal molecular subtypes (Figure 6A).

To validate the above results, the publicly available TCGA RNA-seq data were explored by performing exon junction reads using computational spliced transcripts alignment to a reference (STAR) method to determine *FGFR2* isoform status in 387 EEC patients. There was inconsistency in the proportion of the four *FGFR2b/c* groups in this

Table 2. Univariable Cox regression survival analyses in EEC of the Vancouver cohort

Variables [Ref]	OS			DSS			PFS					
	Events/total	HR	95% CI	P value	Events/total	HR	95% CI	P value	Events/total	HR	95% CI	P value
Age ≥ 60 [age < 60]	127/343	2.51	1.68–3.79	0.0001	63/279	2.05	1.12–3.73	0.02	47/278	1.12	0.63–2.01	0.696
BMI > 30 [BMI ≤ 30]	102/299	1.19	0.774–1.84	0.423	44/244	1.27	0.699–2.29	0.436	41/246	1.37	0.74–2.52	0.321
Myo invasion ≥50% [<50%]	126/339	2.14	1.50–3.04	0.0001	51/264	4.27	2.352–7.76	0.0001	45/274	4.11	2.22–7.60	0.0001
LVI+ [LVI–]	123/323	2.03	1.36–3.05	0.0001	47/264	3.67	2.02–6.68	0.0001	40/263	3.40	1.79–6.45	0.0001
Grade 3 [grade 1/2]	126/342	2.09	1.39–3.14	0.0001	54/268	3.87	2.09–7.20	0.0001	45/275	3.93	2.01–7.67	0.0001
FIGO stage III/IV [I/II]	125/338	2.222	1.403–3.52	0.001	52/265	3.58	2.05–6.25	0.0001	45/274	4.00	2.199–7.27	0.0001
ER expression–low [high]	126/334	1.12	0.071–2.35	0.202	54/276	1.15	0.74–2.87	0.121	45/272	5.34	2.23–20.18	0.151
PR expression–low [high]	125/335	1.09	0.65–1.89	0.388	55/277	1.02	0.63–2.69	0.103	47/271	4.28	2.20–14.80	0.004
Molecular subtype	127/343			0.0001	55/268			0.004	47/274			0.032
POLE [p53wt]		0.62	0.29–1.28	0.195		0.33	1.26–4.09	0.007		0.20	0.027–1.51	0.119
MMRd [p53wt]		2.01	1.32–3.04	0.001		2.27	0.08–1.41	0.135		2.03	0.79–5.17	0.14
p53abn [p53wt]		2.028	1.29–4.01	0.005		2.35	1.02–5.41	0.045		0.75	0.41–1.35	0.330
ESMO risk group	127/338			0.0001	54/268			0.0001	45/275			0.0001
ESMO risk intermediate [low]		1.28	0.741–2.22	0.376		2.06	0.78–5.43	0.145		1.238	0.38–4.07	0.725
ESMO risk high [low]		2.51	1.58–3.98	0.0001		6.80	3.01–15.38	0.0001		8.247	3.44–19.77	0.0001
FGFR2 isoform status	105/295			0.016	55/268			0.0052	47/278			0.038
FGFR2b+/FGFR2c– [FGFR2b–/FGFR2c+]		0.48	0.30–0.78	0.003		0.31	0.15–0.62	0.001		0.265	0.15–0.42	0.019
FGFR2b+/FGFR2c [FGFR2b–/FGFR2c+]		1.03	0.61–1.74	0.924		0.82	0.41–1.63	0.566		0.785	0.56–1.76	0.082
FGFR2b–/FGFR2c– [FGFR2b–/FGFR2c+]		0.83	0.47–1.48	0.534		0.67	0.30–1.49	0.326		0.857	0.57–1.67	0.807

P values of <0.05 are indicated in bold. Cases with missing value are removed from analysis. BMI, body mass index; ESMO, ESMO endometrial cancer risk group; Myo, myometrial; p53, tumor suppressor protein 53; p53abn, null/missense p53 mutation; p53wt, wild-type p53.

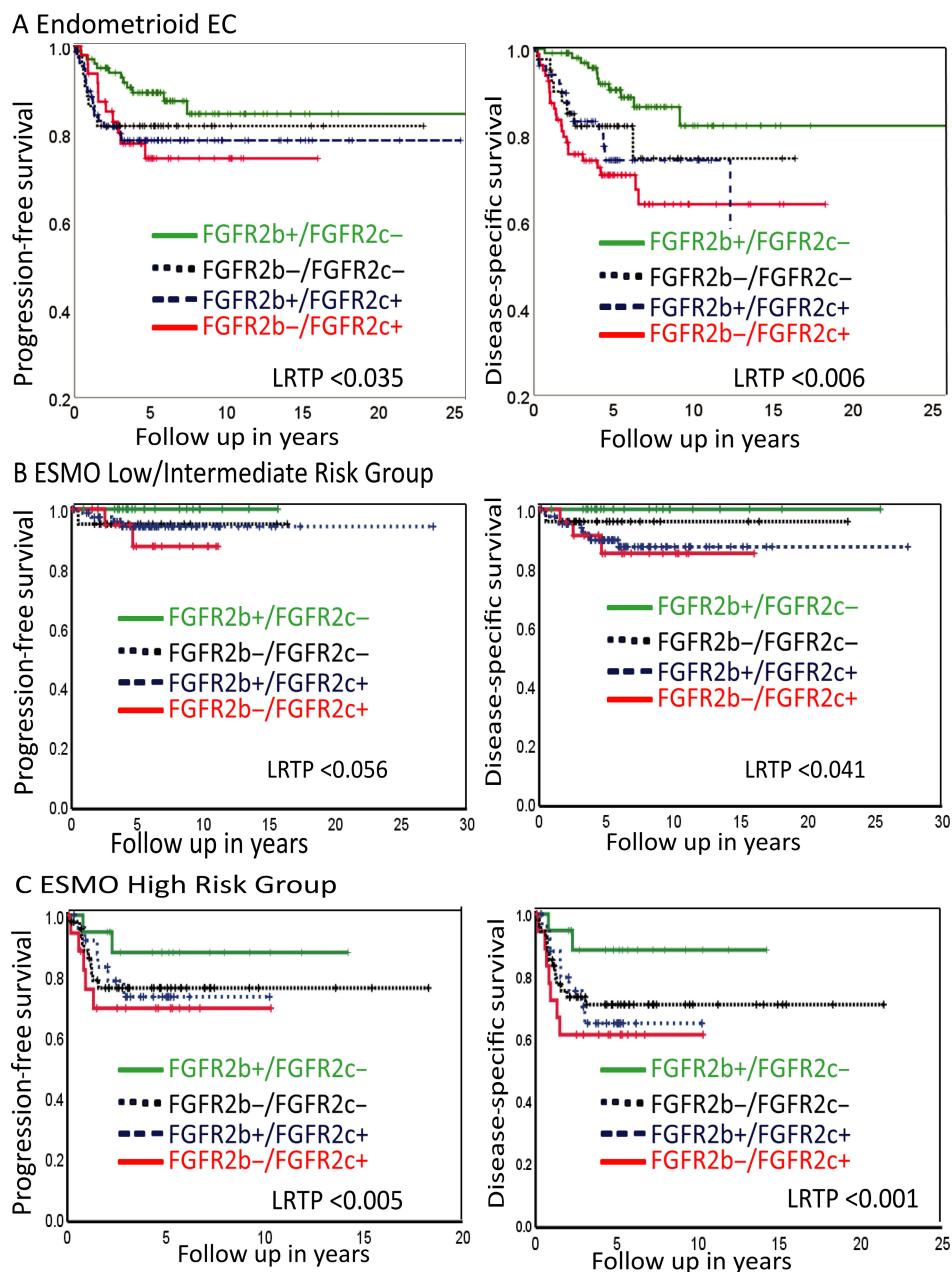


Figure 5. Kaplan–Meier curves of PFS and DSS in EEC of the Vancouver cohort. (A) Analyses in the EEC without stratifying by risk group. Analyses performed stratifying by ESMO risk group: (B) low/intermediate- and (C) high-risk group.

TCGA cohort compared to the Vancouver cohort. *FGFR2b+/FGFR2c-* expression was documented in 291/387 (75%), *FGFR2b-/FGFR2c-* in 67/387 (17%), *FGFR2b+/FGFR2c+* in 6/387 (2%), and *FGFR2b-/FGFR2c+* in 23/387 (6%). *FGFR2b+/FGFR2c-* expression was associated with well-differentiated tumors, early stage, and more common in copy-number low/p53wt molecular subtype in EEC which is consistent with the

finding in the Vancouver cohort (supplementary material, Table S3). Kaplan–Meier curve and Cox regression analyses also showed that *FGFR2b+/FGFR2c-* tumors had longer PFS compared with *FGFR2b-/FGFR2c+* tumors in EEC patients in the TCGA cohort (supplementary material, Table S4 and Figure 6B). Finally, we analyzed the TCGA RNA-seq data to determine patterns of gene expression after supervised clustering by *FGFR2* isoform status.

Table 3. Multivariate Cox regression survival analyses in EEC of the Vancouver cohort

Variables [reference]	HR	95% CI	L RTP
OS			
Age ≥ 60 [age < 60]	1.85	1.08–2.58	0.045
LVI [LVI–]	1.742	1.087–2.792	0.021
Myo invasion >50% [Myo invasion ≤50%]	1.998	1.265–3.157	0.003
Molecular subtype			0.051
POLE [p53wt]	0.37	0.144–0.954	0.04
MMRd [p53wt]	1.378	0.843–2.252	0.201
p53abn [p53wt]	1.077	0.497–2.336	0.851
<i>FGFR2</i> isoform status			0.02
<i>FGFR2b+</i> / <i>FGFR2c</i> – [<i>FGFR2b</i> –/ <i>FGFR2c+</i>]	0.71	0.409–0.921	0.045
<i>FGFR2b+</i> / <i>FGFR2c+</i> [<i>FGFR2b</i> –/ <i>FGFR2c+</i>]	1.80	0.996–3.340	0.052
<i>FGFR2b</i> –/ <i>FGFR2c</i> – [<i>FGFR2b</i> –/ <i>FGFR2c+</i>]	1.23	0.648–2.349	0.523
DSS			
LVI [LVI–]	2.932	1.492–5.762	0.002
Molecular subtype			0.036
MMRd [p53wt]	1.723	0.855–3.473	0.128
POLE [p53wt]	0.22	0.05–0.972	0.046
p53abn [p53wt]	1.565	0.504–4.86	0.438
ESMO risk group			0.0001
Intermediate [low]	1.192	0.379–3.746	0.764
High [low]	4.102	1.601–10.511	0.003
<i>FGFR2</i> isoform status			0.036
<i>FGFR2b+</i> / <i>FGFR2c</i> – [<i>FGFR2b</i> –/ <i>FGFR2c+</i>]	0.37	0.153–0.872	0.023
<i>FGFR2b+</i> / <i>FGFR2c+</i> [<i>FGFR2b</i> –/ <i>FGFR2c+</i>]	0.67	0.495–0.972	0.054
<i>FGFR2b</i> –/ <i>FGFR2c</i> – [<i>FGFR2b</i> –/ <i>FGFR2c+</i>]	0.95	0.398–1.366	0.794
PFS			
Myo invasion >50% [no Myo invasion or ≤50%]	2.70	1.33–5.46	0.006
Grade 3 [grade 1–2]	2.89	1.40–5.97	0.004
Molecular subtype			0.057
POLE [p53wt]	0.21	0.051–1.672	0.068
MMRd [p53wt]	1.91	1.21–3.21	0.017
P53abn [p53wt]	3.20	2.12–4.65	0.052
<i>FGFR2</i> isoform status			0.051
<i>FGFR2b+</i> / <i>FGFR2c</i> – [<i>FGFR2b</i> –/ <i>FGFR2c+</i>]	0.592	0.263–1.087	0.075
<i>FGFR2b+</i> / <i>FGFR2c+</i> [<i>FGFR2b</i> –/ <i>FGFR2c+</i>]	0.76	0.463–2.09	0.147
<i>FGFR2b</i> –/ <i>FGFR2c</i> – [<i>FGFR2b</i> –/ <i>FGFR2c+</i>]	0.978	0.762–2.33	0.887

P values of <0.05 are indicated in bold. Cases with missing value are removed from analysis.

BMI, body mass index; ESMO, ESMO endometrial cancer risk group; Myo, myometrial; p53, tumor protein 53; p53abn, null/misense p53 mutation; p53wt, wild-type p53; L RTP, log-rank test *P* value.

As expected, ECs with *FGFR2b+*/*FGFR2c*– expression showed higher expression of multiple epithelial markers including E-cadherin, hormone receptors (ER and PR), and expression of *FGFR2b*-binding ligands (FGF3 and FGF7), whereas those ECs with *FGFR2b*–/*FGFR2c+* expression showed characteristic expression of mesenchymal markers (such as CDH2). *FGFR2b*–/*FGFR2c+* expressing ECs also showed high expression of *FGFR2c* cognate ligands (FGF2, FGF9, and FGF18) (supplementary material, Figure S2).

ESRP1 regulates *FGFR2* splicing by binding to upstream intronic sequences and repressing the inclusion of the mesenchymal-specific exon, and loss of ESRP1 is associated with epithelial-to-mesenchymal transition (EMT) [26–28]. Lower *ESRP1* expression was observed in tumors expressing *FGFR2c* (supplementary material,

Figure S2). Therefore, we investigated the association of *ESRP1* expression with the four classes of *FGFR2* isoform expression. Notably, *ESRP1* expression was significantly higher in those tumors expressing the *FGFR2b+*/*FGFR2c*– than *FGFR2b*–/*FGFR2c+* tumors (supplementary material, Figure S3).

Discussion

FGFR2 is one of the prototypic genes where alternative splicing is under tight cell/tissue-specific control under normal physiologic conditions. *FGFR2*/*FGF* signaling is context dependent and contributes to different physiologic and pathologic roles in different tissues.

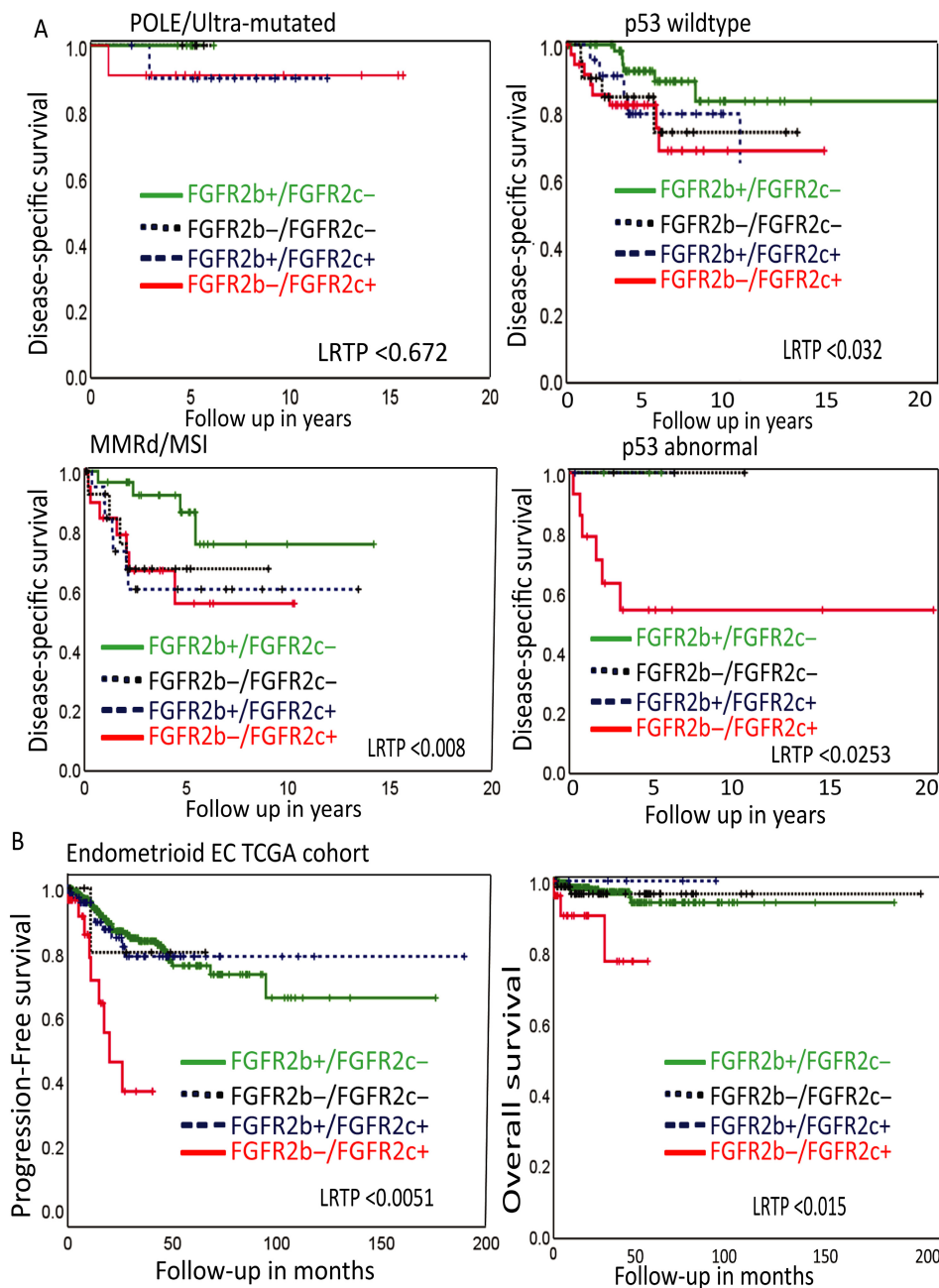


Figure 6. Kaplan–Meier curve survival outcome analyses in the Vancouver and TCGA cohorts according to *FGFR2* isoform status. (A) DSS in the Vancouver cohort when analyses were performed stratifying by molecular subtypes. (B) PFS and OS in the TCGA cohort, EEC only.

To better understand the temporal and spatial expression of *FGFR2b* and *FGFR2c* isoforms in EC tumor progression, we first evaluated the pattern of *FGFR2b* and *FGFR2c* expression in apparently normal endometrium at different cyclic phases in reproductive-aged women, in atrophic endometrium from postmenopausal women, and in hyperplasia with and without

atypia. For the first time, we have clearly demonstrated the correct context of morphologic localization of the two *FGFR2* isoforms in secretory phase, proliferative phase, and atrophic normal endometrium. We observed the *FGFR2b+ / FGFR2c–* pattern of expression in the epithelial cells of normal endometrium in women at different cyclic phases. Previously, Peng *et al* reported

FGFR2c expression in the normal epithelial compartment using IHC [29]. Our novel BaseScope RNA ISH assay, which we have shown previously to be very specific and sensitive [11], suggests that the antibody used in the previous report was not completely specific. Although Peng *et al* showed the antibody used did not detect FGFR2b using western blotting, they did not rule out the potential cross-reactivity with FGFR1b/c [29]. We noted high *FGFR2b* expression in the secretory endometrium in the epithelial compartment but lower expression in proliferative endometrium and very low signals in atrophic endometrium. Our findings are consistent with the previous report by Gatius *et al* who found high FGFR2 protein expression in secretory phase endometrium using a non-isoform-specific pan-FGFR2 antibody [19]. The secretory phase is characterized by increased vascularization and epithelial differentiation and a surge in blood progesterone supporting previous data indicating cross-talk between PR and FGFR2b signaling [30].

We also observed *FGFR2b+/FGFR2c-* isoform expression in women with hyperplasia without atypia which has a low risk of progression to EEC (1–3%) if left untreated [31]. *FGFR2b* expression was also observed in the epithelial compartment of hyperplasia with atypia. A unique pattern of *FGFR2c* isoform expression was seen in a subset of hyperplasia with atypia with some positive signals at the base of the lesion, perhaps correlating with tumor-initiating stem cells [32]. Patients with hyperplasia with atypia are at higher risk of progression to EC (~30–40%) if left untreated [31]. Development of EEC involves a series of hyperplastic changes; however, it is not well understood what drives transformation and progression of hyperplasia to EEC. FGFR2c has been implicated in several hallmarks of cancer including proliferation, uncontrolled tumor growth, migration, invasion, EMT [26], and stemness [33], but whether FGFR2b to FGFR2c isoform switching drives early tumor transformation in EEC requires more mechanistic investigation.

Previously, we reported that the expression of *FGFR2c* splice isoform was associated with aggressive tumor characteristics and poor survival outcome [11] as well as progestin treatment failure in a separate cohort of women [20]. In this former study, tumors with expression of *FGFR2c* were compared to all those not expressing *FGFR2c* (including those that had lost both *FGFR2b* and *FGFR2c* expression) [11]. The current study used *FGFR2b* expression to break down *FGFR2* expression into four groups: those with *FGFR2b-/FGFR2c+* (mesenchymal phenotype); those with *FGFR2b+/FGFR2c-* (epithelial phenotype); those with *FGFR2b+/FGFR2c+* (hybrid phenotype); and those without expression (*FGFR2b-/FGFR2c-*) and showed that these groups have differing prognoses.

Nearly 48% of the screening cohort and 35% of EEC patients in the Vancouver cohort had the *FGFR2b+/FGFR2c-* expression pattern indicating their tumors had not undergone isoform switching. We found a much higher proportion (~75%) of *FGFR2b+/FGFR2c-* expression in the TCGA cohort. These differences are likely due to the increased sensitivity of RNA ISH which could detect subclonal *FGFR2b/FGFR2c* expression compared to computational methods using RNA-seq data on bulk tumors. In addition, it may also reflect that the samples in the discovery and Vancouver cohorts were collected from tertiary referral hospitals and thus included a higher number of high-risk EC cases.

Notably, *FGFR2b+/FGFR2c-* expression was strongly associated with favorable prognostic factors including well-differentiated histology, superficial myometrial invasion, higher PR/ER expression, and low/intermediate risk group, and was more common in the p53wt molecular subtype. On the other hand, EEC patients with either partial (*FGFR2b+/FGFR2c+*) or complete isoform switching (patients with *FGFR2b-/FGFR2c+*) had more aggressive tumor characteristics. Loss of expression of both *FGFR2* isoforms was more common in grade 3 tumors with deep myometrial invasion, indicating loss of *FGFR2* expression or isoform switching may each act as potential mechanisms of tumor progression in EEC.

Cox regression analyses also revealed that EEC patients with *FGFR2b+/FGFR2c-* expression had a better prognostic outcome compared to *FGFR2b-/FGFR2c+* tumors. Both univariable and multivariable Cox regression analyses showed that women with *FGFR2b+/FGFR2c-* expression have longer DSS compared with those expressing *FGFR2b-/FGFR2c+*. The low/intermediate-risk group patients with *FGFR2b+/FGFR2c-* expression were nearly all free of events and, even in the high-risk group, EEC patients with *FGFR2b+/FGFR2c-* expression had longer PFS and DSS. Patients with tumors expressing both isoforms (*FGFR2b+/FGFR2c+*) and those patients without expression (*FGFR2b-/FGFR2c-*) showed a mixed prognosis with a trend to poor prognosis that overlapped with that of *FGFR2b-/FGFR2c+* tumors. Our result is consistent with a previous report that showed *FGFR2b* expression is associated with small tumor size, grade 1/2, node negative, and early-stage tumors in clear cell renal cell carcinoma [14]. Teles *et al* also reported that FGFR2b and high ESRP1 (FGFR2b main splice regulator protein) co-expression associated with favorable tumor profiles and better survival outcome in gastric cancer [34], consistent with our findings. ESRP1 suppresses EMT and potentially inhibits tumor metastasis through maintaining the expression of FGFR2b (epithelial isoform). Our study also supports the notion that FGFR2b and FGFR2c have distinct signaling pathways to regulate

tumor behavior and phenotype when stimulated by their cognate FGF ligands [35].

In our initial report, we proposed that *FGFR2c* expression could be used as a poor prognosis biomarker. Based on the current analysis showing poorer prognosis in the ~10% of EECs that do not express either isoform, we propose that the *FGFR2b+/FGFR2c-* pattern of expression could be used to identify those women with improved survival for de-escalation of treatment, especially within the p53wt and MMRd molecular subtypes. Although the numbers were small, *FGFR2b+/FGFR2c-* tumors were also identified in six patients within the p53 mutant subtype with no events, suggesting *FGFR2b+/FGFR2c-* expression may also be able to identify those patients whose tumors have not undergone EMT and have a low risk of progression. Those patients with *FGFR2b+/FGFR2c-* expression could potentially be managed with less extensive surgical staging that predisposes to further complications such as lymphedema and potentially less aggressive adjuvant treatment. The main limitation of the current study is that it was performed in a retrospective cohort from a single institution and thus this finding requires validation in additional retrospective or prospective patient cohorts. There are two major clinical trials testing de-escalation of treatment in specific molecular cohorts including the PORTEC 4A phase III clinical trial (NCT03469674) in Europe [8] and the TAPER phase II trial (NCT04705649) in Canada [36]. The current data suggest that additional patients showing *FGFR2b+/FGFR2c-* expression may also be eligible for de-escalation of treatment.

There are several clinical trials initiated or completed to target FGFR-dysregulated solid cancers including *FGFR2* alterations (amplification/over expression, fusion, or mutations) [37–40]. Pooled analyses from these clinical trials showed that amplification or fusion alone could not predict treatment response [41]. This indicates that better predictive biomarkers are still needed for FGFR precision targeted therapy. Indeed, *FGFR2* isoform status may play a role in predicting response to FGFR inhibitors in several solid cancer types [42].

In conclusion, *FGFR2b* is expressed in the epithelial compartment of normal endometrium and hyperplasia without atypia and *FGFR2c* is occasionally expressed in the peri-glandular stroma. Notably, *FGFR2b+/FGFR2c-* expression is associated with favorable clinicopathologic prognostic biomarkers and very good survival outcomes. If FGFR inhibition were ever to be tested or implemented in the adjuvant treatment setting, then evaluation of both *FGFR2* isoforms could guide risk stratification (for the 80% of ECs that fall

within the MMRd and p53wt subtypes), with consideration of precision adjuvant therapy for those patients with *FGFR2c*-expressing tumors. We propose that, even in the absence of anti-FGFR therapies, *FGFR2b+/FGFR2c-* expression is a marker of an ‘epithelial like’ tumor with indolent tumor characteristics that could be used to identify patients within the ESMO intermediate/high-risk group for de-escalation of treatment. This finding needs validation in additional retrospective cohorts and ultimately evaluation in a prospective clinical trial before implementing in clinical practice.

Acknowledgements

The authors would like to thank to all patients for their generous support of providing their samples for this investigation. We are also grateful to the QUT histology core facility members at Kelvin Grove, TRI histology core facility, and TRI microscopy facility for whole slide scanning and other technical support. The Translational Research Institute (TRI) Australia receives support from the Australian Government, Department of Health. The study was funded by Cancer Australia (1087165). The funders have no role in study conception, design, data collection, analysis, interpretation, or writing.

Author contributions statement

ATS contributed to conceptualization, methodology development, data curation, statistical analysis, investigation, visualization and manuscript writing – original draft, review and editing. DS, CES, SL, AT, EDW and JNM were involved in data curation, resources, investigation and manuscript – review and editing. PMP contributed to conceptualization, methodology development, investigation, resources, manuscript writing, review and editing, funding acquisition and supervision of the study. All authors have read the final version and agreed to submission and publication in its current version.

References

1. Bray F, Ferlay J, Soerjomataram I, et al. Global cancer statistics 2018: GLOBOCAN estimates of incidence and mortality worldwide for 36 cancers in 185 countries. *CA Cancer J Clin* 2018; **68**: 394–424.
2. Bokhman JV. Two pathogenetic types of endometrial carcinoma. *Gynecol Oncol* 1983; **15**: 10–17.

3. Levine D, The Cancer Genome Atlas Research Network. Integrated genomic characterization of endometrial carcinoma. *Nature* 2013; **497**: 67–73.
4. Stelloo E, Bosse T, Nout RA, et al. Refining prognosis and identifying targetable pathways for high-risk endometrial cancer; a TransPORTEC initiative. *Mod Pathol* 2015; **28**: 836–844.
5. Stelloo E, Nout RA, Osse EM, et al. Improved risk assessment by integrating molecular and clinicopathological factors in early-stage endometrial cancer – combined analysis of the PORTEC cohorts. *Clin Cancer Res* 2016; **22**: 4215–4224.
6. Talhouk A, McConechy MK, Leung S, et al. A clinically applicable molecular-based classification for endometrial cancers. *Br J Cancer* 2015; **113**: 299–310.
7. Talhouk A, McConechy MK, Leung S, et al. Confirmation of ProMise: a simple, genomics-based clinical classifier for endometrial cancer. *Cancer* 2017; **123**: 802–813.
8. van den Heerik ASVM, Horeweg N, Nout RA, et al. PORTEC-4a: international randomized trial of molecular profile-based adjuvant treatment for women with high-intermediate risk endometrial cancer. *Int J Gynecol Cancer* 2020; **30**: 2002–2007.
9. Babina IS, Turner NC. Advances and challenges in targeting FGFR signalling in cancer. *Nat Rev Cancer* 2017; **17**: 318–332.
10. Helsten T, Elkin S, Arthur E, et al. The FGFR landscape in cancer: analysis of 4,853 tumors by next-generation sequencing. *Clin Cancer Res* 2016; **22**: 259–267.
11. Sengal AT, Patch A-M, Snell CE, et al. FGFR2c mesenchymal isoform expression is associated with poor prognosis and further refines risk stratification within endometrial cancer molecular subtypes. *Clin Cancer Res* 2020; **26**: 4569–4580.
12. Ricol D, Cappellen D, El Marjou A, et al. Tumour suppressive properties of fibroblast growth factor receptor 2-IIIb in human bladder cancer. *Oncogene* 1999; **18**: 7234–7243.
13. Amann T, Bataille F, Spruss T, et al. Reduced expression of fibroblast growth factor receptor 2IIIb in hepatocellular carcinoma induces a more aggressive growth. *Am J Pathol* 2010; **176**: 1433–1442.
14. Zhao Q, Caballero OL, Davis ID, et al. Tumor-specific isoform switch of the fibroblast growth factor receptor 2 underlies the mesenchymal and malignant phenotypes of clear cell renal cell carcinomas. *Clin Cancer Res* 2013; **19**: 2460–2472.
15. Grose R, Fantl V, Werner S, et al. The role of fibroblast growth factor receptor 2b in skin homeostasis and cancer development. *EMBO J* 2007; **26**: 1268–1278.
16. Filant J, DeMayo FG, Pru JK, et al. Fibroblast growth factor receptor two (FGFR2) regulates uterine integrity and fertility in mice. *Bio Repro* 2014; **90**: 7.
17. FIGO Committee on Gynaecologic Oncology. Revised FIGO staging for carcinoma of the endometrium. *Int J Gynaecol Obstet* 2009; **105**: 103–104.
18. McShane LM, Altman DG, Sauerbrei W, et al. REporting recommendations for tumor MARKer prognostic studies (REMARK). *Nat Clin Pract Urol* 2005; **2**: 416–422.
19. Gatius S, Velasco A, Azueta A, et al. FGFR2 alterations in endometrial carcinoma. *Mod Pathol* 2011; **24**: 1500–1510.
20. Sengal AT, Smith D, Rogers R, et al. Fibroblast growth factor receptor 2 isoforms detected via novel RNA ISH as predictive biomarkers for progestin therapy in atypical hyperplasia and low-grade endometrial cancer. *Cancers* 2021; **13**: 1703.
21. Abouhashem NS, Ibrahim DA, Mohamed AM. Prognostic implications of epithelial to mesenchymal transition related proteins (E-cadherin, Snail) and hypoxia inducible factor 1 α in endometrioid endometrial carcinoma. *Ann Diagn Pathol* 2016; **22**: 1–11.
22. Tanaka Y, Terai Y, Kawaguchi H, et al. Prognostic impact of EMT (epithelial-mesenchymal-transition)-related protein expression in endometrial cancer. *Cancer Biol Ther* 2013; **14**: 13–19.
23. Thiery JP, Acloque H, Huang RYJ, et al. Epithelial-mesenchymal transitions in development and disease. *Cell* 2009; **139**: 871–890.
24. Eisen MB, Spellman PT, Brown PO, et al. Cluster analysis and display of genome-wide expression patterns. *Proc Natl Acad Sci U S A* 1998; **95**: 14863–14868.
25. Pollock PM, Gartside MG, Dejeza LC, et al. Frequent activating FGFR2 mutations in endometrial carcinomas parallel germline mutations associated with craniosynostosis and skeletal dysplasia syndromes. *Oncogene* 2007; **26**: 7158–7162.
26. Warzecha CC, Sato TK, Nabet B, et al. ESRP1 and ESRP2 are epithelial cell-type-specific regulators of FGFR2 splicing. *Mol Cell* 2009; **33**: 591–601.
27. Götgens EL, Span PN, Zegers MM. Roles and regulation of epithelial splicing regulatory proteins 1 and 2 in epithelial-mesenchymal transition. In: *International Review of Cell and Molecular Biology*, Jeon KW, Galluzzi L (Eds). Cambridge: Academic Press. 2016; 163–194.
28. Warzecha CC, Shen S, Xing Y, et al. The epithelial splicing factors ESRP1 and ESRP2 positively and negatively regulate diverse types of alternative splicing events. *RNA Biol* 2009; **6**: 546–562.
29. Peng WX, Kudo M, Fujii T, et al. Altered expression of fibroblast growth factor receptor 2 isoform IIIc: relevance to endometrioid adenocarcinoma carcinogenesis and histological differentiation. *Int J Clin Exp Pathol* 2014; **7**: 1069–1076.
30. Li Q, Kannan A, DeMayo FJ, et al. The antiproliferative action of progesterone in uterine epithelium is mediated by Hand2. *Science* 2011; **331**: 912–916.
31. Kurman RJ, Kaminski PF, Norris HJ. The behavior of endometrial hyperplasia. A long-term study of "untreated" hyperplasia in 170 patients. *Cancer* 1985; **56**: 403–412.
32. Cousins FL, O DF, Gargett CE. Endometrial stem/progenitor cells and their role in the pathogenesis of endometriosis. *Best Pract Res Clin Obstet Gynaecol* 2018; **50**: 27–38.
33. Kim S, Dubrovskaya A, Salamone RJ, et al. FGFR2 promotes breast tumorigenicity through maintenance of breast tumor-initiating cells. *PLoS One* 2013; **8**: e51671.
34. Teles SP, Oliveira P, Ferreira M, et al. Integrated analysis of structural variation and RNA expression of FGFR2 and its splicing modulator ESRP1 highlight the ESRP1^{amp}-FGFR2^{norm}-FGFR2-IIIc^{high} axis in diffuse gastric cancer. *Cancers* 2020; **12**: 70.
35. Yin Y, Ornitz DM. FGF9 and FGF10 activate distinct signaling pathways to direct lung epithelial specification and branching. *Sci Signal* 2020; **13**: eaay4353.
36. McAlpine J. Tailored Adjuvant Therapy in POLE-mutated and p53-wildtype Early Stage Endometrial Cancer (TAPER). 2021.

- [Accessed 21 November 2021]. Available from: <https://clinicaltrials.gov/ct2/show/NCT04705649>
37. Loria Y, Necchi A, Park SH, *et al.* Erdafitinib in locally advanced or metastatic urothelial carcinoma. *N Engl J Med* 2019; **25**: 338–348.
 38. Kim S-B, Meric-Bernstam F, Kalyan A, *et al.* First-in-human phase I study of aprutumab ixadotin, a fibroblast growth factor receptor 2 antibody-drug conjugate (BAY 1187982) in patients with advanced cancer. *Target Oncol* 2019; **14**: 591–601.
 39. Gilbert JA. BGI398 for FGFR-altered advanced cholangiocarcinoma. *Lancet Oncol* 2018; **19**: e16.
 40. Javle M, Lowery M, Shroff RT, *et al.* Phase II study of BGI398 in patients with FGFR-altered advanced cholangiocarcinoma. *J Clin Oncol* 2018; **36**: 276–282.
 41. Silverman IM, Hollebecque A, Friboulet L, *et al.* Clinicogenomic analysis of FGFR2-rearranged cholangiocarcinoma identifies correlates of response and mechanisms of resistance to pemigatinib. *Cancer Discov* 2021; **11**: 326–339.
 42. Epstein RJ, Tian LJ, Gu YF. 2b or not 2b: how opposing FGF receptor splice variants are blocking progress in precision oncology. *J Oncol* 2021; **2021**: 9955456.

SUPPLEMENTARY MATERIAL ONLINE

Figure S1. Representative micrography showing *FGFR2b* expression in apparently normal human cervical and colon epithelia

Figure S2. Heat map showing the pattern of gene expression according to the *FGFR2* isoform status in the TCGA UCEC cohort

Figure S3. Box plot showing mRNA expression of *ESRP1* according to the *FGFR2* isoform status in EEC from the TCGA cohort

Table S1. Association of *FGFR2* isoform status with clinicopathologic prognostic markers

Table S2. Pairwise multiple comparisons of survival outcomes among the four patterns of *FGFR2* isoform expression of EEC in the Vancouver cohort

Table S3. Association between *FGFR2* isoform status and clinicopathologic and molecular subtypes in EEC in the TCGA cohort

Table S4. Univariable and multivariable Cox regression analyses of PFS within EEC in the TCGA cohort